



Hyperfine Fields at the Cd Site in $\text{La}_{0.67}\text{Cd}_{0.25}\text{MnO}_3$ CMR Manganites

J. P. ARAÚJO^{1,3,*}, J. G. CORREIA^{2,3}, V. S. AMARAL^{1,4}, P. B. TAVARES^{5,6},
F. LENCART-SILVA⁵, A. A. C. S. LOURENÇO⁴, J. B. SOUSA¹, J. M. VIEIRA⁶,
J. C. SOARES² and the ISOLDE Collaboration³

¹*IFIMUP, Universidade do Porto, Rua do Campo Alegre, 687, 4150 Porto, Portugal;*
e-mail: joao.araujo@cern.ch

²*ITN, E.N. 10, P-2685 Sacavém, Portugal*

³*CERN-EP, CH 1211 Genève 23, Switzerland*

⁴*Dep. de Física, Universidade de Aveiro, 3810 Aveiro, Portugal*

⁵*Secção de Química, Universidade de Trás-os-Montes e Alto Douro, 5000 Vila Real, Portugal*

⁶*Dep. de Engenharia Cerâmica e Vidro, Universidade de Aveiro, 3810 Aveiro, Portugal*

⁷*CFNUL, Av. Prof. Gama Pinto No 2, 1699 Lisboa Codex, Portugal*

(Received: 13 July 2000)

Abstract. Although Cd and Ca ions have the same valence and cation size, their incorporation into vacancy-doped La manganites induce different properties. While the incorporation of Ca leads to high T_c up to 250 K and induces a metallic-like behaviour, the incorporation of Cd severely reduces T_c and promotes insulator-like behaviour. In this work, the Cd hyperfine fields have been measured with the Perturbed Angular Correlations (PAC) technique after implantation and annealing of ^{111m}Cd in La–Cd–MnO₃ samples. The PAC results are compared with measurements of the resistivity and magnetization performed on the same samples. The mixed La and Mn site Cd occupancy is suggested as a possibility to explain the properties of the La–Cd–MnO₃ system.

Key words: double exchange, magnetic oxides, colossal magnetoresistance, PAC.

1. Introduction

Nowadays, intense experimental [1] and theoretical [2] research programs are being devoted to the class of oxide materials which shows large changes of the electrical resistivity as a function of an applied magnetic field. The so-called Colossal Magnetoresistive (CMR) manganese oxides, often referred to as manganites, have crystal structures derived from the cubic perovskite ABO₃, where Mn occupies the B site and rare-earth lanthanides (La, Pr, Nd, ...) occupy the A site. Doping is often achieved by the substitution of the trivalent ion by divalent ions (Ca, Sr, Ba, Pb, ...).

In the particular case of the antiferromagnetic LaMnO₃ compound, the effectiveness of the doping is commonly related with the ionic size of the La-substituting

* Corresponding author.

divalent ion. Thus, the Ca^{2+} and Cd^{2+} doped manganites are expected to have similar transport and magnetic properties, once their ionic radii are very similar (0.134 and 0.131 nm, respectively). In addition, one would expect similar T_c , around 267 K, for 33% Cd or Ca substitution. However, the experimental situation is much more controversial. Usual CMR metallic-like ferromagnetic behaviour and $T_c \sim 250$ K were first reported [3] for bulk and thin film $\text{La}_{0.67}\text{Cd}_{0.33}\text{MnO}_3$, in agreement with the above supposition. In contrast, recent studies performed in bulk $\text{La}_{1-x}\text{Cd}_x\text{MnO}_3$ [4–6] indicate that the Cd doping leads to a ferromagnetic insulator-like behaviour, the CMR features being observed at a much lower $T_c \sim 150$ K for $x \sim 0.35$. Since in [3] no chemical analysis is reported and no comments were made about the incorporation of the highly volatile Cd, we attempt the possibility that in their work mainly the vacancy-doped $\text{La}_{0.67}\text{MnO}_3$ was produced, which has similar properties as the compound Ca 33% doped system [6].

So far, two scenarios are proposed to explain the Cd doping features:

- (i) Cd substitutes Mn and disrupts the Mn–O–Mn double-exchange interaction, similarly to the effects of other transition metal like Fe, Cu, Zn, . . . , or
- (ii) Cd substitutes La but promotes a charge redistribution that leads to ferromagnetic superexchange interactions Mn–O–Mn and insulating behaviour.

In this work we present preliminary studies of the magnetic and quadrupole hyperfine fields at ^{111}Cd nuclei, which were performed with the Perturbed Angular Correlations (PAC) technique and combined with resistivity and magnetisation measurements on La–Cd– MnO_3 and La–Ca– MnO_3 samples.

2. Experimental

Pellet samples were prepared from a stoichiometric mixture of La_2O_3 , CdCO_3 (or CaCO_3) and MnO_2 powders. To reduce cadmium losses, the reactants were calcinated for 24 h at low temperature (700°C). The powder mixture was then annealed at 900°C and 1200°C in 24 h steps, to be finally sintered at 1300°C for 10 h in air. Atomic Absorption Spectroscopy (AAS) and Energy Dispersive Spectrometry (EDS) checked the sample's compositions.

$\text{La}_{0.67}\text{Cd}_{0.25}\text{MnO}_3$ samples were implanted at room temperature (RT) with ^{111m}Cd ($T_{1/2} = 48$ min) to a dose of $1.0 \cdot 10^{13}$ at/cm² and 60 keV energy at the ISOLDE facility [7]. ^{111m}Cd decays to the $5/2 + 245$ keV probing state of ^{111}Cd . γ – γ and e^- – γ PAC experiments were performed on a 4-BaF₂-detector spectrometer [8] and on a Kleinheinz–Siegbahn spectrometer equipped with two-magnetic lens and two BaF₂ detectors [9], respectively. The as-implanted $^{111m}\text{Cd}/^{111}\text{Cd}$ e^- – γ PAC spectra (not presented in this paper) are highly attenuated due to the fact that the implanted Cd nuclei are interacting with randomly distributed implantation defects. Best annealing conditions were found for furnace annealing at 973 K, during 20 min in 1 bar flowing oxygen. The fits to the $R(t)$ experimental PAC functions are calculated numerically, by taking into account the full Hamiltonian for the nuclear quadrupole and magnetic combined interactions [10].

3. Results and discussion

Figure 1 shows the temperature dependence of the resistivity (top) and of the magnetization (bottom) for two samples with the same content of Cd and Ca (25%). Both samples are ferromagnetic ($\text{La}_{0.75}\text{Ca}_{0.25}\text{MnO}_3$, $T_c = 235$ K and $\text{La}_{0.67}\text{Cd}_{0.25}\text{MnO}_3$, $T_c = 148$ K) but the Cd doped samples show an insulator-like behaviour over all the temperature range (only a small anomaly in resistivity is present at 148 K), whereas in the Ca doped sample the expected insulator–metal transition is observed. This illustrates that although Ca and Cd have a similar ionic radius they induce very different properties when incorporated into manganites. The fact that the Cd samples are 8% vacancy doped hints, in particular, that T_c should be even more reduced if the La concentration would achieve 75%, thus enhancing the differences on the doping characteristics of Cd and Ca doped manganites.

Figure 2 shows the $^{111m}\text{Cd}/^{111}\text{Cd}$ γ - γ PAC spectra measured after annealing at (a) 300 K, (b) 200 K and (c) 10 K. The room-temperature spectrum was fitted (continuous lines at the spectra) assuming that mainly two fractions $f_1 = 85 \pm 5\%$ and $f_2 = 15 \pm 5\%$ of Cd nuclei interact with two different EFG₁ and EFG₂ distributions, respectively, which are assumed to be Lorentzian-like. EFG₁ is characterised by $\langle \nu_{Q1} \rangle = 224 \pm 5$ MHz with Full Width at Half-Maximum

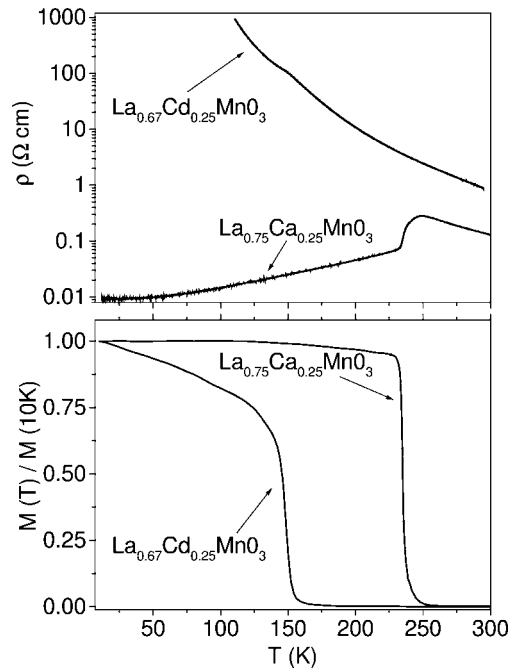


Figure 1. Comparison of the temperature dependence of the resistivity (top) and of the magnetization (bottom) for $\text{La}_{0.75}\text{Ca}_{0.25}\text{MnO}_3$ and $\text{La}_{0.67}\text{Cd}_{0.25}\text{MnO}_3$. Magnetization curves are normalized to unit at 10 K.

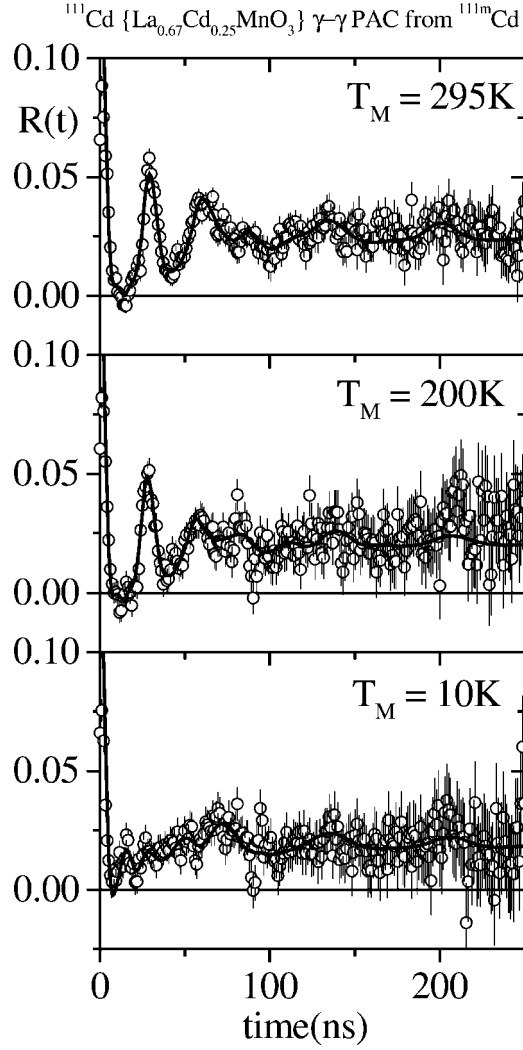


Figure 2. γ - γ PAC spectra measured after implantation of $^{111\text{m}}\text{Cd}$ and 20 min, 973 K flowing O_2 annealing measured at room temperature, 200 K and 10 K.

$\text{FWHM}_{Q1} = 55 \pm 2$ MHz and $\langle \eta_1 \rangle = 0.13 \pm 0.02$. EFG_2 is characterised by $\langle \nu_{Q2} \rangle = 100 \pm 5$ MHz with $\text{FWHM}_{Q2} = 4.4 \pm 0.8$ MHz and $\langle \eta_2 \rangle \sim 0$. We believe that the origin of these distributions is mainly due to the random cation and vacancy distribution always present on the doped materials. By taking the ratio $R = V_{zz}/(1 - \gamma_\infty)$, where $(1 - \gamma_\infty)$ is the Sternheimer antishielding coefficient that accounts for the EFG enhancement due to the polarisation of the probe's electronic core [15], we find for EFG_1 , $R_1 = 3.81 \pm 0.14$ V/Å².

At 200 K (Figure 2(b)) EFG_1 and EFG_2 are still characterised by similar parameters, with $f_1 = 85 \pm 5\%$, $\langle \nu_{Q1} \rangle = 234 \pm 5$ MHz, $\text{FWHM}_{Q1} = 60 \pm 2$ MHz,

$\langle \eta_1 \rangle = 0.13 \pm 0.02$, $f_2 = 15 \pm 5\%$, $\langle \nu_{Q2} \rangle = 97 \pm 5$ MHz, $\text{FWHM}_{Q2} = 10 \pm 2$ MHz and $\langle \eta_2 \rangle \sim 0$.

In a different way, Figure 2(c) clearly shows that at 10 K the $R(t)$ function has drastically changed, looking much more attenuated. To fit this spectrum, the same fit parameters that characterise the EFG₁ and EFG₂ quadrupole distributions at 200 K have been used and kept constant. The best fit considers that only the fraction f_1 of ¹¹¹Cd nuclei interact now with a magnetic hyperfine field (MHF₁) in addition to the EFG₁ distribution, that is characterised by $\omega_L = 50(3)$ Mrad/s with an angle $\beta = 48(5)$ between the MHF and the EFG₁ (V_{zz}) principal direction. We believe that the magnetic field measured by PAC at 10 K, $\text{MHF}_1 = 3.38 \pm 0.2$ T, is related with the ferromagnetic order occurring at temperatures below $T_c = 148$ K in $\text{La}_{0.67}\text{Cd}_{0.25}\text{MnO}_3$, as shown in Figure 1. This was recently confirmed by PAC experiments, which show the onset of the magnetic field at temperatures around T_c [16].

Rasera *et al.* [18] have measured the quadrupole and magnetic hyperfine fields of Ta in the undoped LaMnO_3 using the ¹⁸¹Hf/¹⁸¹Ta PAC probe. In their work, a combined magnetic-quadrupole interaction was also found at low temperatures obtaining, respectively, a Sternheimer normalised ratio $R_{\text{Rasera}} \sim 2.86 \pm 0.09$ V/Å² and $\text{MHF}_{\text{Rasera}} = 3.48 \pm 0.03$ T (10 K). These authors assumed the Hf/Ta nuclei to be at the Mn site, based on the assumption that if Ta would sit on a La site the Ta(La)–O–Mn bond angle would be 90° and consequently very little spin density could be transferred from the Mn ions to the La/Ta site. Thus, the high MHF value is only compatible with the Ta lying at the Mn site where the Mn–O–Mn angle approaches 180°.

In spite of the fact that the materials used in this work are Cd doped, differently from the ones used in [18] and that the scaling of EFGs by using Sternheimer coefficients of impurities with very different electronic structures can lead to false interpretations, once that R_1 and MHF_1 are similar to R_{Rasera} and $\text{MHF}_{\text{Rasera}}$ we hint that the implanted Cd ions mostly go to the same Hf/Ta site. If Rasera and Catchen arguments hold, such a high MHF measured with ¹¹¹Cd in $\text{La}_{0.67}\text{Cd}_{0.25}\text{MnO}_3$ strongly suggest that Cd ions mainly occupies the Mn site.

4. Conclusions

We have shown that below the ferromagnetic Curie temperature ($T_c = 148$ K) an interaction of magnetic origin appears that is observable at the ^{111m}Cd/¹¹¹Cd PAC spectra. Concerning the Cd lattice site location, even if the total incorporation of Cd (25%) at the Mn site appears to be very improbable, double occupancy of Cd in A and B sites could explain the PAC measurements as well as the macroscopic transport properties. Detailed studies of the hyperfine fields are being done on doped materials with various Cd concentrations. These are being further combined with Cd lattice site location studies performed with the emission channeling technique [19].

Acknowledgements

Dr. M. Deicher and Dr. A. Burchard from the Konstanz University are kindly acknowledged for allowing the use of the γ - γ PAC spectrometer where some of the data were obtained. We are grateful to Dr. H. Haas from HMI-Berlin for many useful discussions. J. P. A. and J. G. C. acknowledge scholarships from FCT-PRAXIS XXI/BD/11245/97 and ITN, respectively. This work was funded by the projects CERN/C/FIS/15180/99 and PRAXIS/P/CTM/13142/98.

References

1. Coey, J. M. D. *et al.*, *Adv. Phys.* **48** (1999), 167.
2. Moreo, A., Yunoki, S. and Dagotto, E., *Science* **283** (1999), 2034.
3. Sahana, M. *et al.*, *Appl. Phys. Lett.* **71** (1997), 2701.
4. Troyanchuk, I. O. *et al.*, *J. Phys. Condens. Matter* **10** (1998), 185.
5. Troyanchuk, I. O. *et al.*, *Phys. Status Solidi A* **164** (1997), 821.
6. Araújo, J. P. *et al.*, to be published in *JMMM Proc. of ICM'2000*, 6–11 August 2000, Recife, Brazil.
7. Kugler, E., Fiander, D., Jonson, B., Haas, H., Przewloka, A., Ravn, H. L., Simon, D. J., Zimmer, K. and the ISOLDE Collaboration, *Nucl. Instrum. Methods B* **70** (1992), 41.
8. Forkel-Wirth, D. *et al.*, *Solid Stat. Commun.* **93** (1995), 425.
9. Correia, J. G., Araújo, J. P., Marques, J. G., Ramos, A. R., Melo, A. A., Soares, J.C. and the ISOLDE Collaboration, *Z. Naturforschung A* **55a** (2000), 3.
10. Barradas, N. P., Rots, M., Melo, A. A. and Soares, J. C., *Phys. Rev. B* **47** (1993), 8763.
11. Kugler, E., Fiander, D., Jonson, B., Haas, H., Przewloka, A., Ravn, H. L., Simon, D. J., Zimmer, K. and the ISOLDE Collaboration, *Nucl. Instrum. Methods B* **70** (1992), 41.
12. Forkel-Wirth, D. *et al.*, *Solid Stat. Commun.* **93** (1995), 425.
13. Correia, J. G., Araújo, J. P., Marques, J. G., Ramos, A. R., Melo, A. A., Soares, J. C. and the ISOLDE Collaboration, *Z. Naturforschung A* **55a** (2000), 3.
14. Barradas, N. P., Rots, M., Melo, A. A. and Soares, J. C., *Phys. Rev. B* **47** (1993), 8763.
15. Gupta, R. P. and Sen, S. K., *Phys. Rev. A* **8** (1973), 1169;
Feiock, F. D. and Johnson, W. R., *Phys. Rev.* **187** (1969), 39.
16. Araújo, J. P. *et al.*, to be published.
17. Gupta, R. P. and Sen, S. K., *Phys. Rev. A* **8** (1973), 1169;
Feiock, F. D. and Johnson, W. R., *Phys. Rev.* **187** (1969), 39.
18. Rasera, R. L. and Catchen, G. L., *Phys. Rev. B* **58** (1998), 58.
19. Wahl, U., Correia, J. G., Cardoso, S., Marques, J. G., Vantomme, A., Langouche, G. and the ISOLDE Collaboration, *Nucl. Instrum. Methods B* **136–138** (1998), 744.